

Stromal reaction inhibitor and immune-checkpoint inhibitor combination therapy attenuates excluded-type colorectal cancer in a mouse model

Naoki Yorita^a, Ryo Yuge^{b,*}, Hidehiko Takigawa^b, Atsushi Ono^a, Toshio Kuwai^d, Kazuya Kuraoka^e, Yasuhiko Kitadai^c, Shinji Tanaka^b, Kazuaki Chayama^a

^a Department of Gastroenterology and Metabolism, Graduate School of Biomedical and Health Sciences, Hiroshima University, Hiroshima, Japan

^b Department of Endoscopy, Hiroshima University Hospital, Hiroshima, Japan

^c Department of Health and Science, Prefectural University of Hiroshima, Hiroshima, Japan

^d Department of Gastroenterology, National Hospital Organization, Kure Medical Center and Chugoku Cancer Center, Kure, Japan

^e Department of Anatomical Pathology, National Hospital Organization Kure Medical Center and Chugoku Cancer Center, Kure, Japan

ARTICLE INFO

Keywords:

Orthotopic mouse model
Tumor phenotype
Imatinib
Anti-PD-1 antibody

ABSTRACT

Despite recent advances in cancer immunotherapy, the efficacy of colorectal cancer (CRC) immunotherapy regimens is limited. This study evaluated the combined effect of an anti-PD-1 antibody and a platelet-derived growth factor receptor inhibitor (imatinib) on CRC progression using an orthotopic transplanted mouse model that reproduced the three histological phenotypes of CRC (inflamed-, excluded-, and desert-type). The frequency of each of these phenotypes in 196 human CRC tissue samples was also evaluated. Excluded-type CRC had the highest frequency in human tissue samples. In the mouse model, imatinib suppressed stromal reaction and increased sensitivity to anti-PD-1 treatment in excluded-type CRC. Antitumor effect was observed in mice with excluded-type tumors only after concomitant administration of anti-PD-1 antibody and imatinib. Immunohistological analysis revealed a reduction in stromal volume and an increase in the number of CD8-positive T cells in the tumor nest following combination therapy. RNA sequencing revealed significant activation of immune-related pathways and suppression of stromal-related pathways in transplanted tumors treated with combination therapy compared with tumors treated with anti-PD-1 antibody monotherapy. This combination therapy may prove effective for CRC cases that are unresponsive to anti-PD-1 antibody monotherapy.

1. Introduction

The discovery of immune-checkpoint inhibitors (ICIs), including the anti-programmed cell death-1 (PD-1) antibody, dramatically advanced immunotherapy in clinical practice [1–4]. However, the benefits of cancer immunotherapy for colon cancer have only been observed in cases with microsatellite instability (MSI) [5,6]. Although there have been attempts to improve treatment efficacy through the concomitant administration of immunotherapy and other drugs [7,8], no highly efficacious combinations for CRC treatment have been discovered.

Tumor tissue consists of cancer cells and various stromal cells, including immune cells [9–11]. Interactions between cancer cells and the stroma are important for our understanding of cancer growth and

progression. Carcinoma-associated fibroblasts (CAFs) are the primary structural components of the stroma. Although secretory factors, including various chemokines and cytokines released by CAFs, reportedly activate antitumor immune responses in various cancers, there are few studies on the relationship between CAFs and the immune-related tumor microenvironment (TME) [12]. Interactions between CAFs and cancer cells facilitate tumor growth and progression; however, the detailed molecular mechanisms remain unclear [13,14]. In colon cancer, stromal fibroblasts proliferate around the tumor nest when cancer cells infiltrate the submucosal tissue in a process known as “stromal reaction” [15]. High-grade malignancy in cancers is correlated with strong stromal reactions [16–18]. The importance of the interaction between stromal cells and cancer cells via the PDGF/PDGFR axis during

Abbreviations: CRC, colorectal carcinoma; PDGFR, platelet-derived growth factor receptor; ICI, immune checkpoint inhibitor; PD-1, programmed cell death-1; MSI, microsatellite instability; CAF, carcinoma-associated fibroblast; TME, tumor microenvironment; GSEA, gene set enrichment analysis; α -SMA, α -smooth muscle actin.

* Corresponding author. Hiroshima University, Hiroshima, 734-8551, Japan.

E-mail address: makapoo@hiroshima-u.ac.jp (R. Yuge).

<https://doi.org/10.1016/j.canlet.2020.10.041>

Received 24 July 2020; Received in revised form 25 September 2020; Accepted 22 October 2020

Available online 28 October 2020

0304-3835/© 2020 Elsevier B.V. All rights reserved.

tumor growth and progression, and that of the high expression of PDGF receptors in human colorectal cancer (CRC) stroma have been reported [14]. Using a colon cancer orthotopic transplanted mouse model, we confirmed in our previous studies that imatinib administration strongly suppresses stromal reactions by inhibiting the PDGF/PDGFR axis in the tumor stroma [13,14]. However, we could not evaluate tumor immunity in these previous studies as we used immunodeficient nude mice.

Because of the importance of TME histology, the present study focused on the histological phenotypes of CRC, namely inflamed-type, excluded-type, and desert-type, which have been recently proposed for the histological classification of cancer immunity [19–21]. However, relatively few studies have classified human CRC according to these phenotypic classifications. In excluded-type cancers, possible mechanisms for inhibiting T-cell penetration into the tumor include physical barriers offered by abnormal cancer structures or vessels [22,23], lack of T-cell-recruiting chemokines [24], and soluble factor inhibitors, such as IL-10 and TGF β [25]. Based on these theories, T-cell recruitment into the tumor nest may be key to overcoming ICI resistance, especially in excluded-type tumors [26]. Therefore, it may be possible to achieve T-cell infiltration into the tumor nest and strengthen the benefits of tumor immune activation by concomitantly administering ICIs with drugs that inhibit stromal reactions.

This study aimed to evaluate the effect of anti-PD-1 antibody and PDGFR inhibitor combination therapy on the TME with respect to CRC

progression by employing an orthotopic transplanted mouse model that reproduced the three histological phenotypes.

2. Materials and methods

2.1. Phenotypic classification of human CRC tissue, focusing on immune cell infiltration

To examine the proportion of the three phenotypes and their association with clinicopathological features, CD8 immunostaining was performed for surgically resected CRC specimens. A total of 196 consecutive patients with colon cancer who underwent surgical resection for CRC between 2013 and 2015 at the Hiroshima University Hospital, Kure Medical Center, and Chugoku Cancer Center (all in Japan) were enrolled. This study was approved by the institutional review board and the ethics committees of the aforementioned institutions. Written informed consent was obtained from the participants.

This retrospective study was approved by the institutional review board and the ethics committees of Hiroshima University.

(No. E-1237) and was performed in accordance with the Declaration of Helsinki and its later amendments.

This retrospective study was approved by the institutional review board and the ethics committees of Hiroshima University.

Formalin-fixed, paraffin-embedded tumor tissues cut into serial 4- μ m

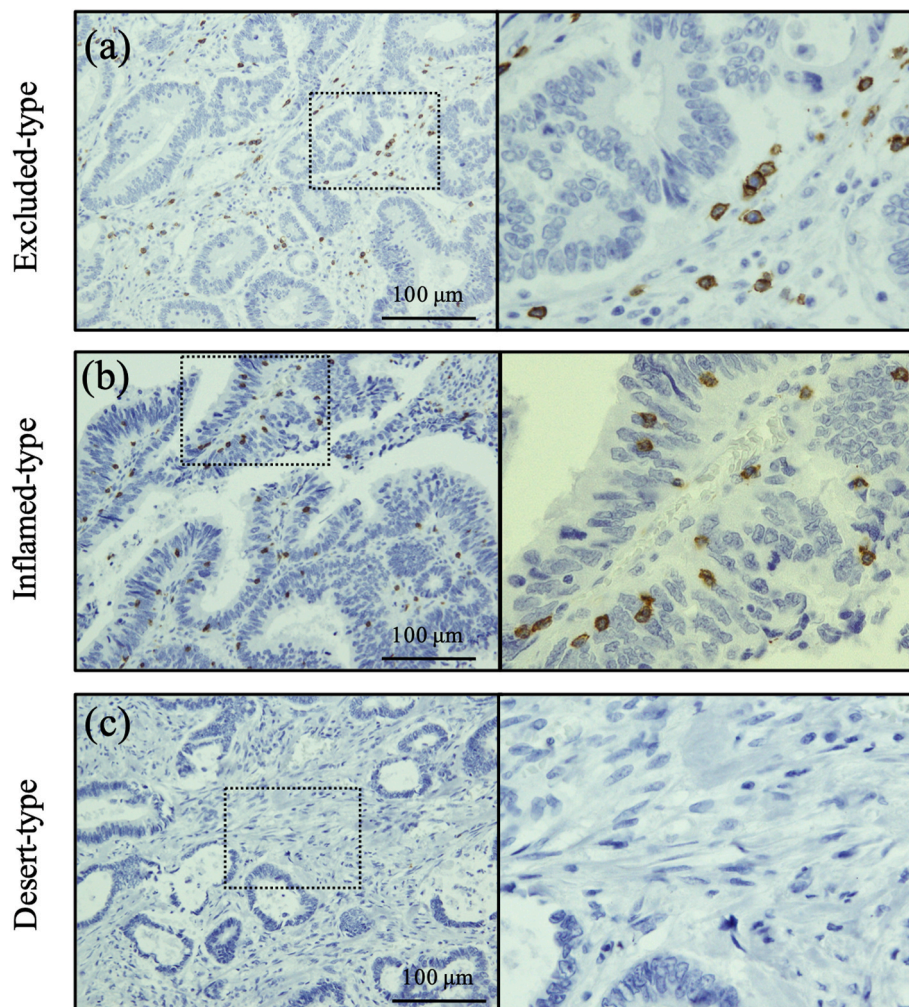


Fig. 1. Representative colorectal cancer cases according to the CD8 immunohistochemistry-based phenotypic classification. (a) Representative image of the inflamed-type tumor; CD8-positive immune cells can be observed in the tumor. (b) Representative image of the excluded-type tumor; CD8-positive immune cells can be observed in the stroma, but not infiltrating the tumor. (c) Representative image of the desert-type tumor; CD8-positive immune cells cannot be observed in the tumor.

sections were examined by immunohistochemistry for CD8 cells as described previously [27]. Immunohistochemistry results were categorized into the three phenotype classifications (Fig. 1) [19–21], after which clinicopathological features among the three groups were compared.

Formalin-fixed, This retrospective study was approved by the institutional review board and the ethics committees of Hiroshima University.

(No. E-1237) and was performed in accordance with the Declaration of Helsinki and its later amendparaffin-embedded tumor tissues cut into serial 4- μ m sections were examined by immunohistochemistry for CD8 cells, as described previously [27]. Immunohistochemistry results were categorized into the three phenotypic classifications as described below (Fig. 1) [19–21] and clinicopathological features among the three groups were compared.

The phenotype classifications include (i) inflamed-type: cases wherein CD8-positive cells infiltrated the cancer cell nest and were in direct contact with cancer cells; (ii) excluded-type: cases wherein CD8-positive cells in the stroma were adjacent to the cancer cell nest but did not directly contact cancer cells; and (iii) desert-type: cases wherein less than 10 CD8-positive cells were observed in five randomly selected microscopic fields at 200 \times magnification.

2.2. Classification of human colon cancer tissue according to microsatellite status

CRC tissue samples were examined for MSI status either by immunohistochemical staining for mismatch repair protein expression or PCR amplification of microsatellite sequences using the resected specimens. MSI determination by PCR was carried out using pentaplex PCR, as described previously [28,29]. Next, the relationship between MSI classification and phenotypic classification was analyzed.

2.3. Culture conditions for mouse colon carcinoma and fibroblast cell lines

CT26, a clonal cell line derived from a BALB/c mouse colon cancer cell line (American Type Culture Collection, Manassas, VA, USA), and JLS-V9, a clonal cell line derived from a BALB/c mouse fibroblast cell line (Riken BRC Cell Bank, Ibaraki, Japan), were used. Cells were maintained in Dulbecco's modified Eagle's medium supplemented with 10% fetal bovine serum (Sigma-Aldrich, St. Louis, MO, USA) and a penicillin-streptomycin mixture.

2.4. Cancer cell proliferation assay

The effects of the interaction between cancer cells and fibroblasts on cell proliferation were compared using a time-lapse assay system (Incucyte; Essen BioScience, Ann Arbor, MI, USA) that automatically measured cell confluence as a percentage over a 5-day period. CT26 (6×10^4 cells/well), JLS-V9 (6×10^4 cells/well), and a co-culture of CT26 cells and JLS-V9 (6×10^4 cells/well) cells were seeded in plates (Essen ImageLock; Essen Bioscience). Anti-PD-1 antibody (1, 5, or 10 nM) or imatinib (1, 2, or 3 μ M) was added to the culture plates. Mouse IgG isotype was used as a control. CT26 cells were easily distinguished from JLS-V9 cells even in co-culture because of green fluorescent protein transfection.

2.5. Animals and orthotopic implantation of tumor cells

Female BALB/c and female athymic nude mice were obtained from Charles River Japan (Tokyo, Japan) and kept under specific pathogen-free conditions. Animal experiments were approved by the Committee on Animal Experimentation of Hiroshima University. All experiments complied with the ARRIVE guidelines and were conducted in accordance with the UK Animals Act, 1986, and the EU Directive 2010/63/EU

for animal experimentation.

To create the inflamed-type CRC mouse model, 1×10^5 CT26 cells in 50 μ L Hank's balanced salt solution (HBSS) were injected into the cecal wall of female BALB/c mice with a zoom stereomicroscope (Carl Zeiss, Oberkochen, Germany). To create the excluded-type CRC mouse model, 1×10^5 CT26 and 1×10^5 JLS-V9 cells in 50 μ L HBSS were injected into the cecal wall of female BALB/c mice. To create the desert-type CRC mouse model, 1×10^5 CT26 cells in 50 μ L HBSS were injected into the cecal wall of female athymic nude mice. The three mouse models were analyzed via immunohistology using α SMA and CD8 to confirm that each type was correctly reproduced.

2.6. Colon cancer treatment of the mouse models

Orthotopic mouse models for evaluating the immune syngeneic response of inflamed-type and excluded-type phenotypes were prepared and treated with anti-PD-1 antibody and imatinib according to the schedule shown in Supplementary Fig. 1. Six days after implantation, the mice were categorized into the following four treatment groups: those administered water daily by oral gavage (control group); those administered 50 mg/kg imatinib per day by oral gavage; those administered 20 mg/kg anti-PD-1 antibody the first day and 10 mg/kg every 6 days by intraperitoneal administration; and those administered a combination of imatinib and anti-PD-1 antibody using the same protocol. The experiment continued for 24 days. On day 25, the mice were euthanized and necropsied.

2.7. Necropsy procedures and histological evaluation

Mice were euthanized, and tumor volume was recorded. Tumor tissues were formalin-fixed, paraffin-embedded, cut into serial 4-mm sections, and then examined by immunohistochemistry for CD8, Ki-67, anti-type I collagen, PD-1, p-PDGFR, and Ki67, as previously reported [30]. The stained area was estimated and the positive cells were enumerated using ImageJ (imagej.nih.gov).

2.8. RNA sequencing and gene set enrichment analysis (GSEA)

Implanted excluded-type tumors treated with anti-PD-1 antibody monotherapy or combination therapy were mechanically dissociated using a homogenizer, following which a RNeasy Mini kit (Qiagen, Hilden, Germany) was used for RNA extraction according to the manufacturer's protocols. Library construction and data processing were performed by Beijing Genomics Institute, China. Libraries were sequenced on a DNBSEQ-G400RS platform, and high-quality reads were aligned to the mouse reference genome (GRCm38). The HOM_Mouse Human Sequence downloaded from the Mouse Genome Informatics website (<http://www.informatics.jax.org/>) was used to convert mouse genes to human genes. After removing the genes with FPKM = 0 from all samples, GSEA was performed as previously described [31] to analyze the differential modulation of molecular pathways.

2.9. Reagents

The anti-PD-1 antibody, 4H2, was procured from Ono-Pharmacy (Osaka, Japan). The primary antibodies used were as follows: monoclonal rabbit anti-CD8 antibody from Abcam (Cambridge, UK); monoclonal mouse anti-PD-1 from Cell Signaling Technology (Danvers, MA, USA); polyclonal rabbit anti-phosphorylated PDGF-R β (p-PDGF-R β) from Santa Cruz Biotechnology (Santa Cruz, CA, USA); rabbit anti- α -smooth muscle actin (α -SMA) from Abcam (Cambridge, UK); Ki-67-equivalent antibody (MIB-1) from Dako (Carpinteria, CA, USA); polyclonal rabbit anti-mouse type I collagen from Novotec (Saint Martin La Garenne, France); imatinib (Gleevec, PDGFR inhibitor) from Novartis Pharma (Basel, Switzerland); and mouse IgG isotype control from bioXcell (Lebanon, NH, USA).

2.10. Statistical analysis

Clinicopathological features were analyzed using the χ^2 test or Fisher’s exact test to compare categorical data, and Student’s *t*-test or Wilcoxon rank sum test was used to compare continuous data. $p < 0.05$ was considered significant. Overall survival rates were calculated using the Kaplan–Meier method. All statistical analyses were performed using JMP software (SAS International Inc., Cary, NC, USA).

3. Results

3.1. Phenotypic classification of human colon cancer tissue

The ratios of the three histological phenotypes in surgically resected human CRC specimens are shown in Table 1. According to phenotypic classification, inflamed-type tumors formed the lowest proportion (9.7%), while excluded-type tumors formed the highest proportion (55.1%). The high frequency of excluded-type tumors suggests that there are many cases of human CRC in which the histological micro-environment makes immunotherapy almost ineffective. Regarding clinicopathological characteristics, patients with inflamed-type tumors were significantly older than those with the other phenotypes. Sex, TNM classification, stage classification, and histological type did not significantly differ between phenotypes. Further, inflamed-type tumors demonstrated a slightly better prognosis than that of other phenotypes; however, the differences were not significant (Fig. 2).

3.2. Classification of human colon cancer tissue according to MSI

Assessment of the relationship between histological phenotype and MSI status showed that 19 of 196 (9.7%) cases demonstrated high MSI (MSI-H). Comparing the proportion of MSI-H CRC cases among the three phenotypes showed that inflamed-type tumors formed the highest proportion (26.3%), with statistical significance (Table 2).

3.3. Effect of an ICI and stromal reaction inhibitor on colon cancer cell lines

Next, the effect of the interaction between cancer cells and stromal cells (fibroblasts), as well as the effects of anti-PD-1 antibodies and a PDGFR inhibitor on cell growth capacity, was compared using a time-lapse system. Comparison of proliferative abilities between cancer

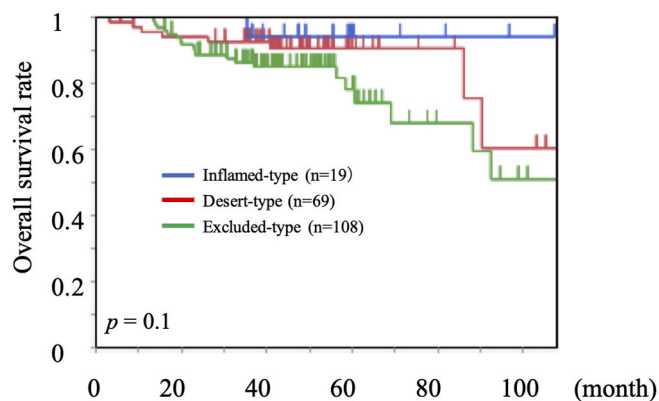


Fig. 2. Survival probability according to the phenotype classification (n = 196). For the survival rate, inflamed-type colorectal cancer tended to show a better prognosis than the other phenotypes, though this was not statistically significant.

Table 2

The relationship between the phenotype classification and the microsatellite status of colorectal cancer cases. (n = 196).

MSI states	Phenotype classification			p-value
	Inflamed-type N = 19	Excluded-type N = 108	Desert-type N = 69	
MSI high	5 (26.3)	9 (8.3)	5 (7.2)	0.03*
MSS	14 (73.7)	99 (91.7)	64 (92.8)	

$P < 0.05$ statistically significant difference, *Inflamed vs Excluded, Inflamed vs Desert.

cells cultured alone and those co-cultured with fibroblasts showed that the proliferative ability of cancer cells was significantly augmented in the co-culture (Fig. 3a). Imatinib did not affect the proliferative capacity of CT26; however, it inhibited JLSV9 proliferative capacity in a dose-dependent manner (Fig. 3b, d). Further, in co-culture, imatinib inhibited the proliferative capacity of CT26 cells in a dose-dependent manner (Fig. 3f). The inhibitory effect of imatinib on cell proliferation was not affected by the addition of anti-PD-1 antibody. (Supplementary Fig. 2.). Anti-PD-1 antibodies did not affect cell proliferation in vitro when immune cells were absent (Fig. 3c, e, g). These results indicate that PDGFR

Table 1

Clinicopathological features and survival rate of colorectal cancers according to the phenotype classification. (n = 196).

variable	Phenotype classification			p-value	
	Inflamed-type n = 19 (9.7%)	Excluded-type n = 108 (55.1%)	Desert-type n = 69 (35.2%)		
Age	73.2 ± 10.8	68.1 ± 10.44	66.8 ± 13.6	0.03*	
Sex	Male	12 (63%)	66 (61%)	36 (52%)	0.4
	Female	7 (37%)	32 (39%)	33 (48%)	
Location	Colon	15 (79%)	83 (78%)	54 (78%)	0.9
	Rectum	4 (21%)	24 (22%)	15 (22%)	
T classification	T1,2	8 (42%)	32 (30%)	21 (30%)	0.5
	T3,4	11 (58%)	76 (70%)	48 (70%)	
N classification	N0	13 (68%)	56 (52%)	31 (45%)	0.2
	N1–3	6 (32%)	52 (48%)	38 (55%)	
M classification	M0	17 (90%)	91 (84%)	53 (77%)	0.3
	M1	2 (11%)	17 (16%)	16 (23%)	
pStage	Stage I, II	13 (68%)	52 (48%)	29 (42%)	0.1
	Stage III, IV	6 (32%)	56 (52%)	40 (58%)	
Lymphatic invasion	Ly0, 1	18 (95%)	91 (84%)	55 (80%)	0.3
	Ly2, 3	1 (5%)	17 (16%)	14 (20%)	
Venous invasion	V0, 1	18 (95%)	94 (87%)	57 (83%)	0.3
	V2, 3	1 (5%)	14 (13%)	12 (17%)	
Histological type	tub1, tub2, pap	17 (89%)	99 (92%)	65 (94%)	0.7
	por, muc	2 (11%)	9 (8%)	4 (6%)	

tub1; well differentiated adenocarcinoma, tub2; moderately differentiated adenocarcinoma, por; poorly differentiated adenocarcinoma, muc; mucinous carcinoma, $P < 0.05$ statistically significant difference, *Inflamed vs Excluded, Inflamed vs Desert.

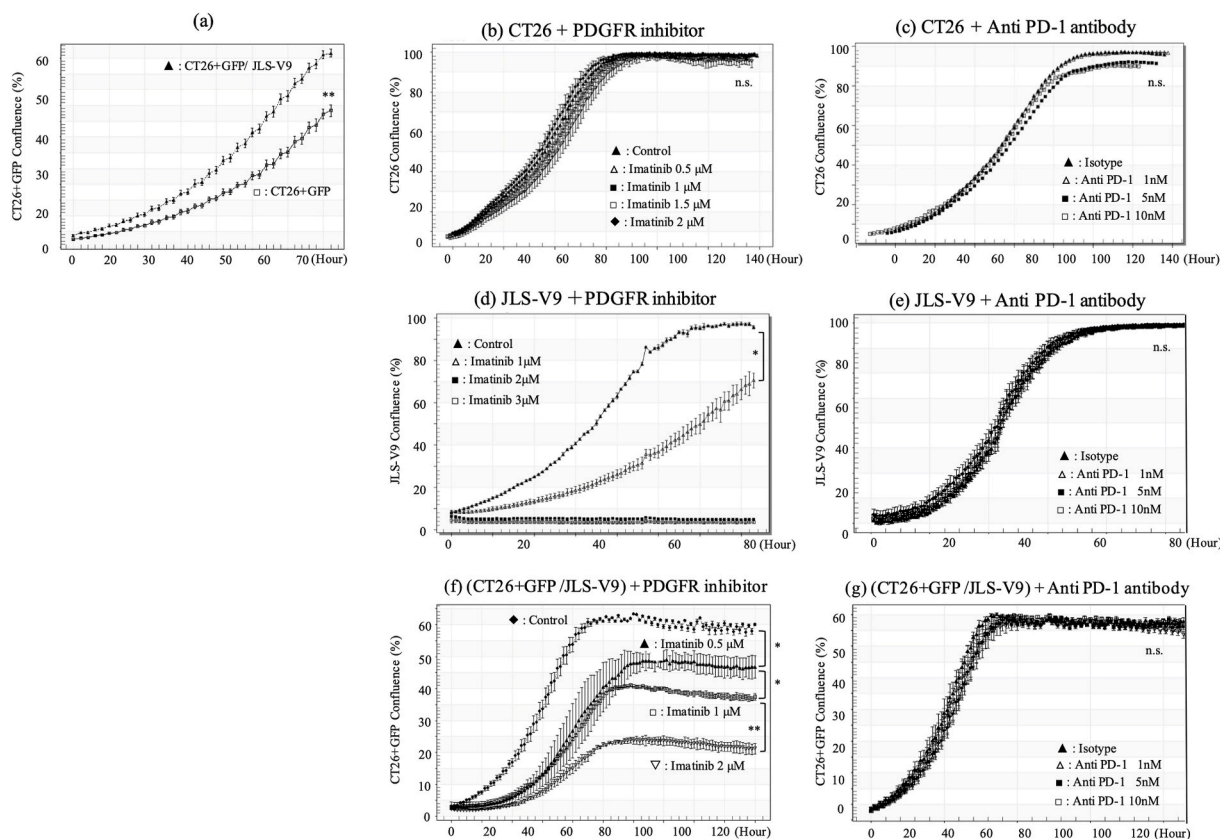


Fig. 3. In vitro cell proliferation assays. (a) Co-culture with JLS-V9 increased the proliferative ability of CT26 cells. (b) The PDGFR inhibitor did not affect the proliferative potential of CT26 cells at clinical concentrations. (c) Anti-PD-1 antibody did not affect the proliferation ability of CT26 cells. (d) PDGFR inhibitor suppressed the proliferative capacity of JLS-V9 cells in a dose-dependent manner. (e) In the JLS-V9 co-culture, administration of the PDGFR inhibitor resulted in a decrease in the proliferative capacity of CT26 cells. (f) Anti-PD-1 antibody did not affect the growth of CT26 cells in the co-culture with JLS-V9 cells. * $p < 0.05$; ** $p < 0.01$.

inhibitor administration suppresses the cell proliferation-promoting effect of fibroblasts and indirectly suppresses cancer cell growth.

3.4. Mouse models of colon cancer according to phenotypic classification

Tumors from each of the orthotopic transplanted mouse models reproducing the three histological phenotypes were analyzed via immunohistology and confirmed to be consistent with each phenotype. In the inflamed-type model, tumors were composed almost exclusively of cancer cells with a sparse stromal reaction and negative immunostaining for α SMA (Fig. 4a and b). In the excluded-type mouse model, stromal reactions among the cancer cell nests were rich and showed strongly positive immunostaining for α SMA. CD8-positive cells were found in the stromal area, but infiltration into the tumor nest was not observed (Fig. 4d and e). Immune cells were positive for PD-1 in both models (Fig. 4c, f). In the desert-type model, histological findings were similar to those of the inflamed-type model, but almost no immune cells were observed (Supplementary Fig. 3).

3.5. Combination therapy for colon cancer growing in the cecal wall

Next, the three orthotopic transplanted mouse models were treated with anti-PD-1 antibodies and a PDGFR inhibitor. A significant reduction in tumor volume was observed with anti-PD-1 antibody monotherapy in the inflamed-type model, whereas combination with the PDGFR inhibitor did not produce a synergistic effect (Fig. 5a). In the excluded-type model, PDGFR and anti-PD-1 antibody combination therapy significantly reduced tumor volume; however, no such decrease was observed with anti-PD-1 antibody monotherapy (Fig. 5b). PDGFR

inhibitor monotherapy did not exert a significant antitumor effect in either model. In the desert-type model, no significant antitumor effect was observed for either monotherapy or combination therapy (Supplementary Fig. 3).

In summary, anti-PD-1 antibody monotherapy was effective in the inflamed-type mouse model, while the synergistic effect of combination treatment was remarkable in the excluded-type mouse model.

3.6. Histopathological analysis of mouse models according to phenotypic classification

To assess the effect of anti-PD-1 antibody and PDGFR inhibitor administered alone or in combination in inflamed- and excluded-type models, tumor sections were immunohistochemically examined for CD8, type I collagen, p-PDGFR, and Ki67.

In the inflamed-type mouse model, there was no significant difference in the number of CD8 cells in the tumor, nor was there a significant difference in the expression levels of type I collagen or p-PDGFR; this was considered to be due to the low stromal reaction in tumors in this model. The expression level of Ki67 was significantly reduced in the anti-PD-1 antibody treatment group (Fig. 6a).

In the excluded-type mouse model, the number of CD8-positive cells in cancer cell nests was low in the control group but increased in the PDGFR inhibitor-administered group. Stromal markers (type I collagen and p-PDGFR) indicated that PDGFR inhibitor administration significantly reduced the stromal reaction. Only the combination therapy group showed a significant decrease in the Ki67 labeling index. These findings imply that in the anti-PD-1 antibody monotherapy group, immune cells cannot infiltrate into tumors because of inhibition by

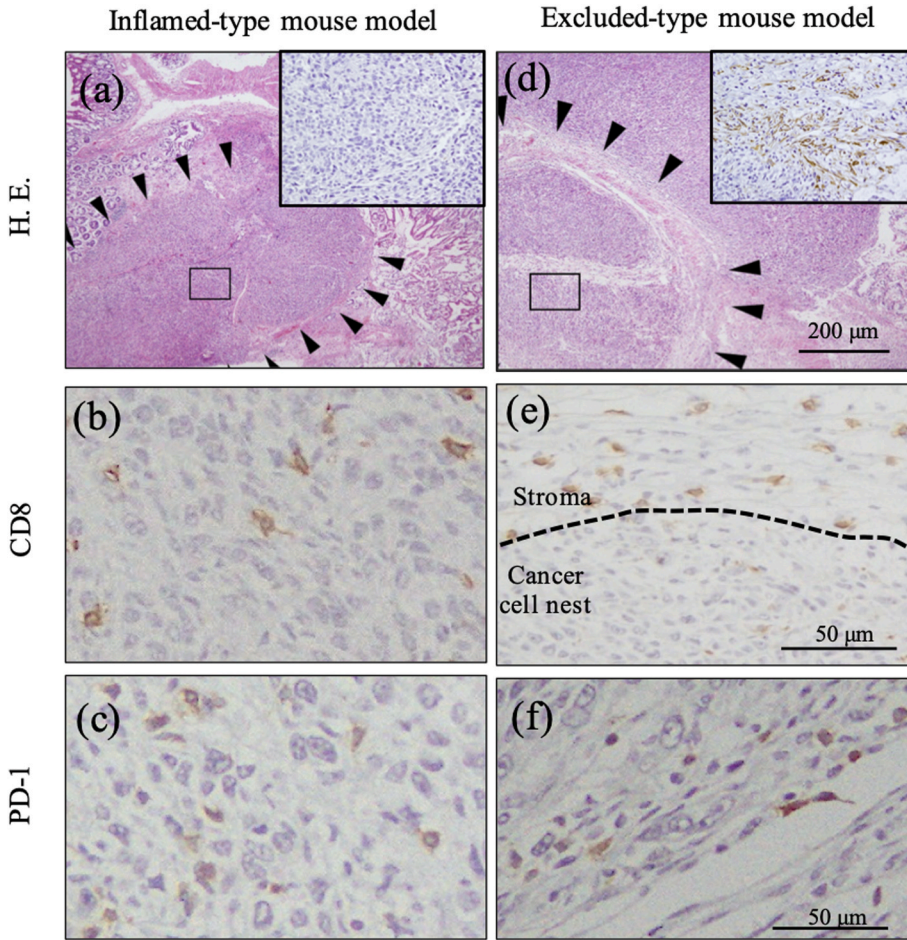


Fig. 4. Histological evaluation of the orthotopically transplanted mouse models reproducing the histological phenotypes. Left column, inflamed-type; right column, excluded-type. (a) The stromal component in the cancer cell nest was scarce, and composed, almost exclusively, of cancer cells in inflamed-type tumors (the region surrounding the arrowhead is the cancer cell nest). Immunohistochemistry of anti- α SMA revealed few fibroblasts in the cancer cell nests (small upper-right window). α SMA: cancer-associated fibroblast marker. (b) Immunohistochemistry of anti-CD8 revealed considerable lymphocyte numbers. (d) Cancer cell nests were surrounded by fibroblasts, and the peri-carcinoma area was abundant in activated fibroblasts in excluded-type tumors (small upper-right window). (e) Lymphocytes were observed abundantly in the stromal region, but not in the cancer cell nests (dotted line indicating the border between cancer cell nests and stroma). (c, f) PD-1 was expressed in immune cells in the tumor.

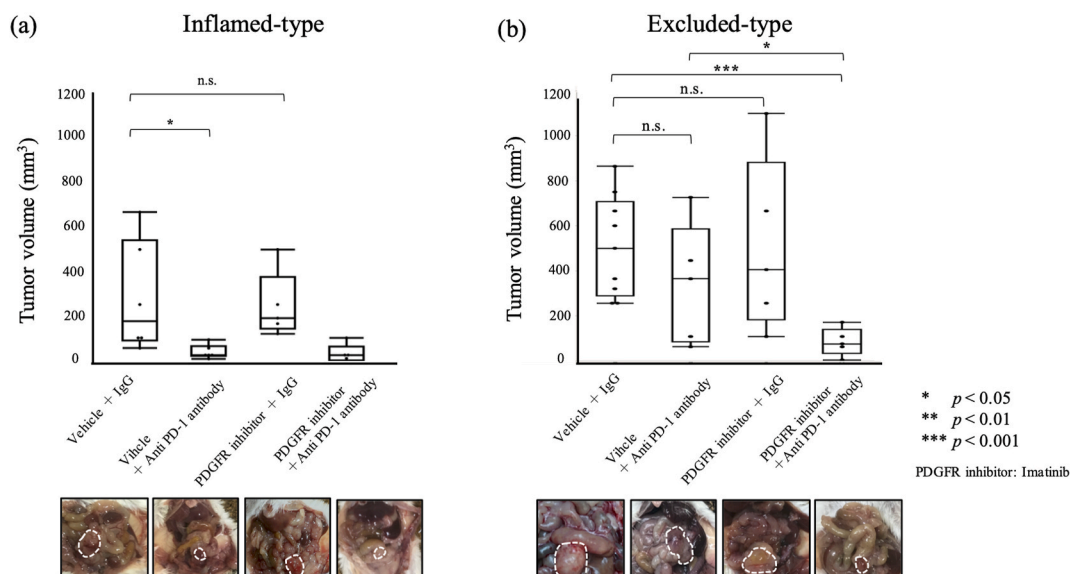
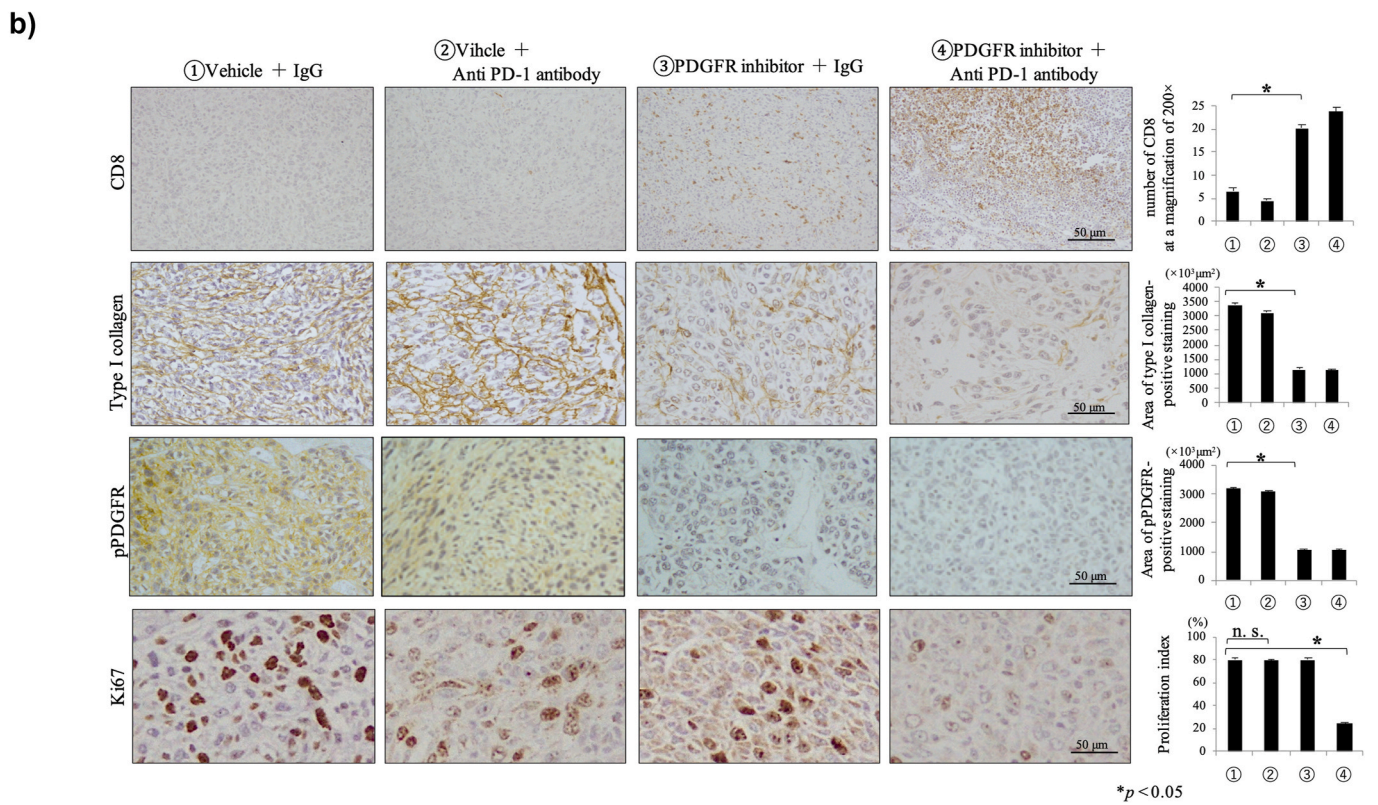
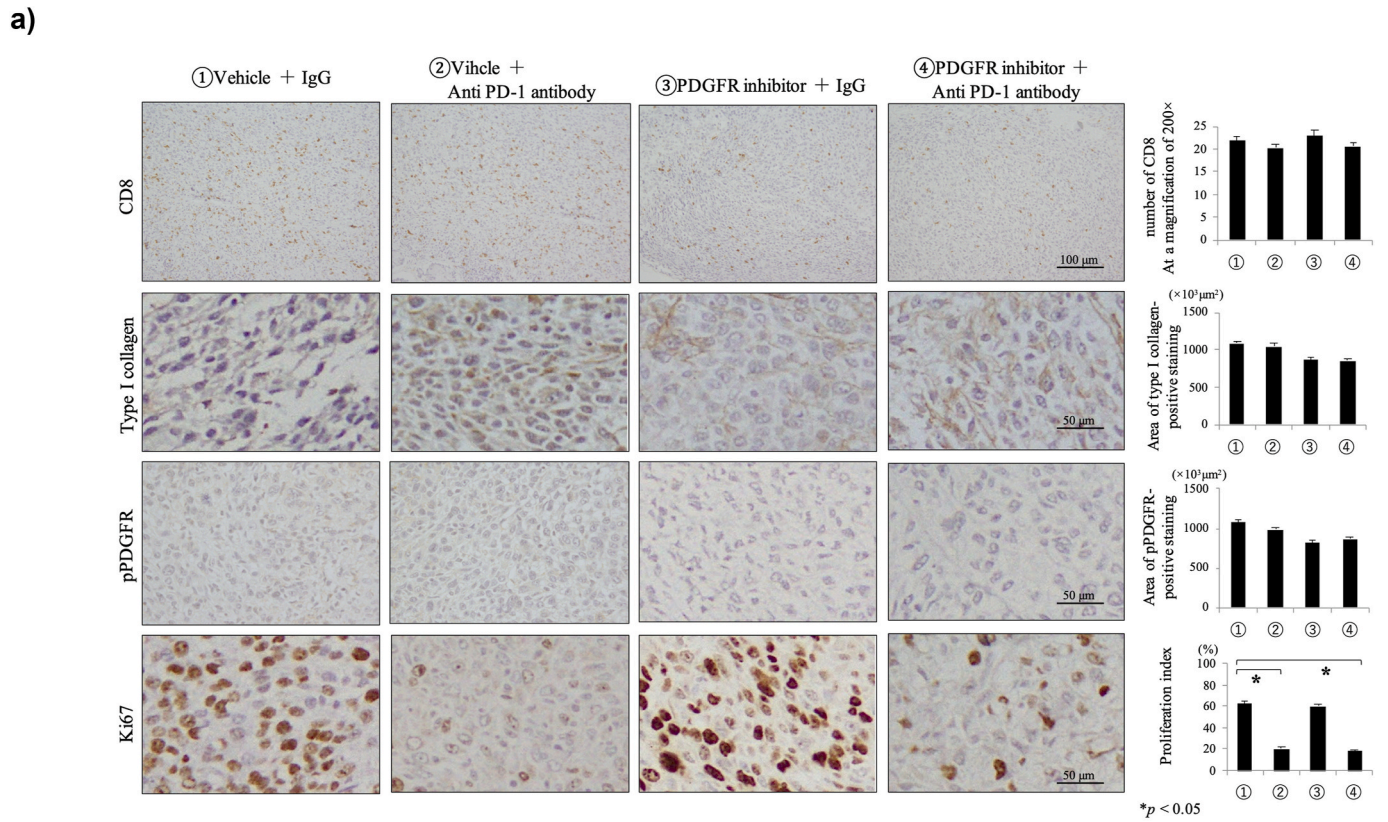


Fig. 5. Tumor volume of the orthotopically implanted tumor at day 25. (a) The therapeutic effect of single anti-PD-1 antibody administration was observed in the inflamed-type model. (b) No antitumor effect was observed with single anti-PD1 antibody administration; only the combination of imatinib and anti-PD1 antibody was effective in the excluded-type tumor model. * $p < 0.05$; ** $p < 0.01$; *** $p < 0.001$. Pictures of the orthotopically implanted tumors are indicated below the bars in each graph.



(caption on next page)

Fig. 6. Immunohistochemical analysis of transplanted tumors. (a) In the inflamed-type transplanted tumor, the positive areas of stromal markers, such as p-PDGFR and type I collagen, did not differ between the groups, and the number of CD8-positive cells in the cancer cell nests did not differ between treatments. Ki67 decreased after treatment with anti-PD-1 antibody, and in the inflamed-type, the anti-PD-1 antibody alone showed antitumor effects. (b) In the excluded-type transplanted tumor, the number of CD8-positive cells in the cancer cell nests was low, and the antitumor effect was not achieved after a single administration of anti-PD-1 antibody. In the imatinib single administration group, stromal volume decreased, and the number of CD8-positive cells increased in the cancer cell nests, but the antitumor effect was not observed. To clarify the localization of PDGFR expression, fluorescent immunostaining was performed (see Supplementary Fig. 4). The antitumor effect was observed after co-administration with the anti-PD-1 antibody. * $p < 0.05$; ** $p < 0.01$.

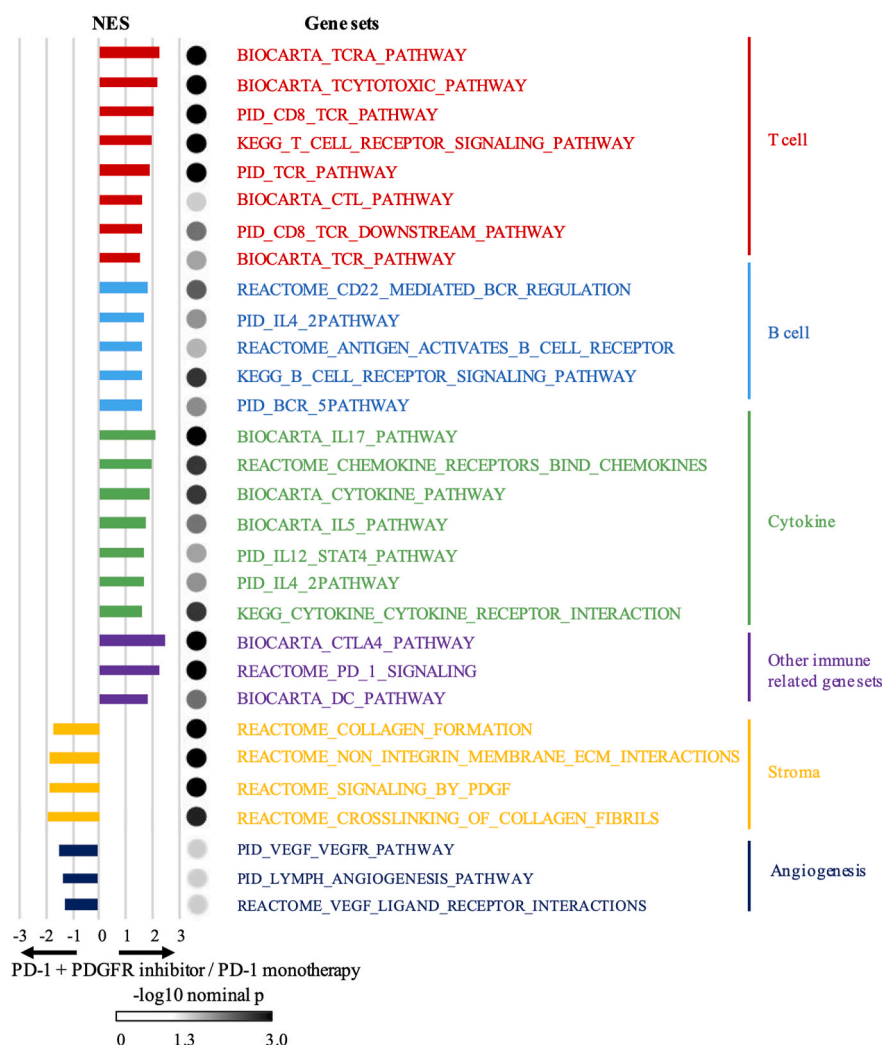


Fig. 7. Summarized GSEA results for significantly (FDR < 0.25) up- or down-regulated, immune- and stroma-related gene sets from the canonical pathways (C2.CP.v7.0). GSEA, gene set enrichment analysis; NES, normalized enrichment score; FDR, false discovery rate.

abundant stromal reactions. However, when the PDGFR inhibitor reduced stromal volume for immune cells to infiltrate into tumors, the antitumor effect of PD-1 was enhanced (Fig. 6b).

3.7. RNA sequencing and GSEA

RNA sequencing was used to comprehensively analyze the changes in tumor immune response in the excluded-type, orthotopically transplanted tumors treated with combination therapy. RNA from implanted tumors treated with anti-PD-1 monotherapy and combination therapy was analyzed using RNA sequencing, following which GSEA was performed to evaluate gene expression and pathway differences. GSEA revealed the enrichment of multiple immune-related pathways, including T-cell-, B-cell-, and cytokine-related pathways, in the combination therapy group compared with the corresponding pathways in the anti-PD-1 monotherapy group. Pathways associated with dendritic cells

in regulating TH1 and TH2 development and the immune checkpoint-related pathway were enriched in the combination therapy group. In contrast, stroma- and angiogenesis related pathways were enriched in the PD-1 monotherapy group. These observations indicate the inhibition of tumor-associated stroma via the blockade of PDGFR signaling pathways and a strong T-cell presence following current combination therapy (Fig. 7).

4. Discussion

Although multiple studies have evaluated various drugs that can be administered concomitantly to improve the benefits of ICI, no high-efficacy combinations have been identified for CRC [7,8]. Furthermore, there are no studies regarding the in vivo relationship between stromal cells and tumor immunity. One reason for this is the difficulty in establishing an in vivo model that reproduces the immune-related TME.

Understanding how cancer stroma affects antitumor immune response is important for the evaluation of animal models in which the TME is reproduced.

Herein, it was revealed that the therapeutic effect of an anti-PD-1 antibody for excluded-type CRC was improved when it was combined with a PDGFR inhibitor. This treatment decreased the stromal reaction and enhanced T-cell infiltration into tumors in an orthotopic transplanted mouse model. The therapeutic effect of an anti-PD-1 antibody is greatly affected by pre-existing T cells, which play an important role in the reactivation of the immunosuppression mechanism [32]. In the TME, one of the mechanisms that allow cancers to evade T cells involves a genetic change to reduce antigenicity and the activation of various oncogenic pathways, such as WNT- β -catenin [33] and JAK-STAT3 [34]. Another mechanism consists of local adaptive immunosuppression caused by checkpoint molecules, such as PD-L1, that are induced by IFN γ released by T cells. Moreover, the TME is marked by a great diversity attributable to various factors, including specific driver mutations and the deregulation of oncogenes in cancer cells [33,34]. Therefore, several complex factors must be assessed to determine their association with T-cell distribution in tumors.

There are currently few studies classifying human CRC according to phenotype [21]. The human CRC immunohistochemistry results from the present study showed that the proportion of patients with inflamed-type CRC was the lowest while that of excluded-type CRC was the highest. These results may reflect the low efficacy of single ICI administration for CRC in clinical practice. Furthermore, altering the characteristics of excluded-type to inflamed-type may be key to increasing the number of patients who respond to immunotherapy. The relationship between MSI status and phenotypic classification of human CRC showed that MSI-H cases were predominant in the inflamed-type model. Therefore, treatment may be effective for MSI-H cases for which immunotherapy is generally successful from the viewpoint of immune cell infiltration [35,36]. Additionally, unstable microsatellite CRCs possess an abundance of immunogenic neoantigens that are recognized by the immune system and contribute to ICI effectiveness [30,37].

PDGFR expression in the stroma is associated with poor prognosis in various cancers, including CRC [38–40]. Increased PDGFR expression levels are reportedly associated with tumor invasion and metastasis in CRC [14]; blocking the signaling pathway with a PDGFR inhibitor is known to effectively suppress angiogenesis and lymphangiogenesis as well as the stromal reaction in mouse models [16,41]. Therefore, the present study used imatinib, a PDGFR inhibitor, as a stromal reaction inhibitor. In solid tumors, high interstitial fluid pressure in stromal cells acts as a barrier to antitumor drugs [42]. Because interstitial fluid pressure is controlled by PDGFR signaling, PDGFR inhibitors decrease interstitial fluid pressure, enhancing the effect of chemotherapy when used in combination [43]. Similarly, imatinib treatment in our study reduced interstitial fluid pressure and may have enhanced the penetration of anti-PD-1 antibodies into the cancer cell nest. Furthermore, these mechanisms are considered to enhance the therapeutic effect of the PD-1 antibody.

This study employed a novel combination therapy of ICI and imatinib to attenuate colon cancer. This research is unique, as it was conducted using orthotopic implanted mouse models with syngeneic immune responses that replicated all three histological phenotypes associated with tumor immunity. The concomitant administration of an ICI and a PDGFR inhibitor resulted in observable antitumor benefits, although the antitumor benefits of ICI monotherapy were not observed in excluded-type tumors (the type commonly observed in colon cancer). PDGFR inhibitor administration suppressed stromal reactions, thereby resolving immunosuppression, and tumor immunity activation was linked to improved ICI benefits. Histologically, suppressing stromal reactions allows immune cells to infiltrate the cancer cell nest, altering the phenotype from excluded-type to inflamed-type; our immunostaining results supported this hypothesis. The GSEA results also supported this

outcome. However, the precise molecular mechanisms underlying these processes are not clearly understood, and further investigation is required.

This study has some limitations. In our in vitro model, we were unable to demonstrate a synergistic effect of the combination of anti-PD1 antibodies and PDGFR inhibitors in the presence of immune cell involvement. Additionally, we used nude mice to express the desert-type, although it is not strictly the same as the physiological desert-type given that there are no thymus-derived T cells to migrate in the nude mouse model. Nevertheless, combination therapy using an ICI and a PDGFR inhibitor was effective for inhibiting tumor growth in excluded-type CRC. This combination therapy may be effective for CRC cases that do not respond to ICI monotherapy.

Credit author statement

Naoki Yorita: Data curation, Investigation Writing - original draft, Ryo Yuge, Funding acquisition Conceptualization, Writing - review & editing, Formal analysis, Hidehiko Takigawa, Methodology, Resources, Validation, Ono Atsushi, Data curation, Toshio Kuwai, Resources, Kazuya Kuraoka, Investigation, Yasuhiko Kitadai, Software, Shinji Tanaka, Visualization, and Kazuaki Chayama, Project administration

Funding

This work was supported by JSPS KAKENHI [grant number JP19K16745].

Declaration of conflict of interest

The authors have no conflicts of interest to disclose.

Acknowledgments

This work was performed with the kind cooperation of the Analysis Center of Life Science and Institute of Laboratory Animal Science (Hiroshima University, Hiroshima, Japan) and the Division of Frontier Medical Science, Department of Surgery, Graduate School of Biomedical Sciences (Hiroshima University, Hiroshima, Japan). We would also like to thank Editage for English language editing.

Appendix A. Supplementary data

Supplementary data to this article can be found online at <https://doi.org/10.1016/j.canlet.2020.10.041>.

References

- [1] J.S. Weber, S.P. D'Angelo, D. Minor, F.S. Hodi, R. Gutzmer, B. Neyns, C. Hoeller, N. I. Khushalani, W.H. Miller, C.D. Lao, G.P. Linette, L. Thomas, P. Lorigan, K. F. Grossmann, J.C. Hassel, M. Maio, M. Sznol, P.A. Ascierto, P. Mohr, B. Chmielowski, A. Bryce, I.M. Svane, J.-J. Grob, A.M. Krackhardt, C. Horak, A. Lambert, A.S. Yang, J. Larkin, Nivolumab versus chemotherapy in patients with advanced melanoma who progressed after anti-CTLA-4 treatment (CheckMate 037): a randomised, controlled, open-label, phase 3 trial, *Lancet Oncol.* 16 (2015) 375–384.
- [2] E.B. Garon, N.A. Rizvi, R. Hui, N. Leighl, A.S. Balmanoukian, J.P. Eder, A. Patnaik, C. Aggarwal, M. Gubens, L. Horn, E. Carcereny, M.-J. Ahn, E. Felip, J.-S. Lee, M. D. Hellmann, O. Hamid, J.W. Goldman, J.-C. Soria, M. Dolled-Filhart, R. Z. Rutledge, J. Zhang, J.K. Lucefor, R. Rangwala, G.M. Lubiniecki, C. Roach, K. Emancipator, Gandhi L for the KEYNOTE-001 Investigators. Pembrolizumab for the treatment of non-small-cell lung cancer, *N. Engl. J. Med.* 372 (2015) 2018–2028.
- [3] H. Borghaei, L. Paz-Ares, L. Horn, D.R. Spigel, M. Steins, N.E. Ready, L.Q. Chow, E. E. Vokes, E. Felip, E. Holgado, F. Barlesi, M. Kohlhaufl, O. Arrietta, M.A. Burgio, FayetteJ, H. Lena, E. Poddubskaaya, D.E. Gerber, S.N. Gettinger, C.M. Rudin, N. Rizvi, L. Crino, G.R. Blumenschein Jr., S.J. Antonia, C. Dorange, C.T. Harbison, F.G. Finckenstein, J.R. Brahmer, Nivolumab versus docetaxel in advanced nonsquamous non-small-cell lung cancer, *N. Engl. J. Med.* 373 (2015) 1627–1639.
- [4] J. Brahmer, K.L. Reckamp, P. Baas, L. Crino, W.E.E. Eberhardt, E. Poddubskaaya, S. Antonia, A. Pluzanski, E.E. Vokes, E. Holgado, D. Waterhouse, N. Ready,

- J. Gainor, O.A. Frontera, L. Havel, M. Steins, M.C. Garassino, J.G. Aerts, M. Domine, L. Paz-Ares, M. Reck, C. Baudelet, C.T. Harbison, B. Lestini, D. R. Spigel, Nivolumab versus docetaxel in advanced squamous-cell non-small-cell lung cancer, *N. Engl. J. Med.* 373 (2015) 123–135.
- [5] Cancer Genome Atlas Network, Comprehensive molecular characterization of human colon and rectal cancer, *Nature* 487 (2012) 330–337.
- [6] R. Gryfe, H. Kim, E.T.K. Hsieh, M.D. Aronson, E.J. Holowaty, S.B. Bull, M. Redston, S. Gallinger, Tumor microsatellite instability and clinical outcome in young patients with colorectal cancer, *N. Engl. J. Med.* 342 (2000) 69–77.
- [7] L. Gandhi, D. Rodríguez-Abreu, S. Gadgeel, E. Esteban, E. Felip, F. De Angelis, M. Domine, P. Clingan, M.J. Hochmair, S.F. Powell, S.Y. Cheng, H.G. Bischoff, N. Peled, F. Grossi, R.R. Jennens, M. Reck, R. Hui, E.B. Garon, M. Boyer, B. Rubio-Viqueira, S. Novello, T. Kurata, J.E. Gray, J. Vida, Z. Wei, J. Yang, H. Raftopoulos, M.C. Pietanza, M.C. Garassino, KEYNOTE-189 investigators. Pembrolizumab plus chemotherapy in metastatic non-small-cell lung cancer, *N. Engl. J. Med.* 378 (2018) 2078–2092.
- [8] C.J. Langer, S.M. Gadgeel, H. Borghaei, V.A. Papadimitrakopoulou, A. Patnaik, S. F. Powell, R.D. Gentzler, R.G. Martins, J.P. Stevenson, S.I. Jalal, A. Panwalkar, J. C. Yang, M. Gubens, L.V. Sequist, M.M. Awad, J. Fiore, Y. Ge, H. Raftopoulos, L. Gandhi, KEYNOTE-021 investigators. Carboplatin and pemetrexed with or without pembrolizumab for advanced, non-squamous non-small-cell lung cancer: a randomised, phase 2 cohort of the open-label KEYNOTE-021 study, *Lancet Oncol.* 17 (2016) 1497–1508.
- [9] G. Bindea, B. Mlecnik, M. Tosolini, A. Kirilovsky, M. Waldner, A.C. Obenauf, H. Angel, T. Fredriksen, L. Lafontaine, A. Berger, P. Bruneval, W.H. Fridman, C. Becker, F. Pages, M.R. Speicher, Z. Trajanoski, J. Galon, Spatiotemporal dynamics of intratumoral immune cells reveal the immune landscape in human cancer, *Immunity* 39 (2013) 782–795.
- [10] J. Galon, A. Costes, F. Sanchez-Cabo, A. Kirilovsky, B. Mlecnik, C. Lagorce-Pages, M. Tosolini, M. Camus, A. Berger, P. Wind, F. Zinzindohoue, P. Bruneval, P.-H. Cugnenc, Z. Trajanoski, W.-H. Fridman, F. Pages, Type, density, and location of immune cells within human colorectal tumors predict clinical outcome, *Science* 313 (2006) 1960–1964.
- [11] F. Pagès, A. Berger, M. Camus, F. Sanchez-Cabo, A. Costes, R. Molitor, B. Mlecnik, A. Kirilovsky, M. Nilsson, D. Damotte, T. Meatchi, P. Bruneval, P.-H. Cugnenc, Z. Trajanoski, W.-H. Fridman, J. Galon, Effector memory T cells, early metastasis, and survival in colorectal cancer, *N. Engl. J. Med.* 353 (2005) 2654–2666.
- [12] L. Ziani, S. Chouaib, J. Thiery, Alteration of the antitumor immune response by cancer-associated fibroblasts, *Front. Immunol.* 9 (2018) 414.
- [13] A. Orimo, P.B. Gupta, D.C. Sgroi, F. Arenzana-Seisdedos, T. Delaunay, R. Naeem, V. J. Carey, A.L. Richardson, R.A. Weinberg, Stromal fibroblasts present in invasive human breast carcinomas promote tumor growth and angiogenesis through elevated SDF-1/CXCL12 secretion, *Cell* 121 (2005) 335–348.
- [14] Y. Kitada, T. Sasaki, T. Kuwai, T. Nakamura, C.D. Bucana, S.R. Hamilton, I. J. Fidler, Expression of activated platelet-derived growth factor receptor in stromal cells of human colon carcinomas is associated with metastatic potential, *Int. J. Canc.* 119 (2006) 2567–2574.
- [15] Olivier De Wever, M. Mareel, Role of tissue stroma in cancer cell invasion, *J. Pathol.* 200 (2003) 429–447.
- [16] R. Yuge, Y. Kitada, K. Shinagawa, M. Onoyama, S. Tanaka, W. Yasui, K. Chayama, mTOR and PDGF pathway blockade inhibits liver metastasis of colorectal cancer by modulating the tumor microenvironment, *Am. J. Pathol.* 185 (2015) 399–408.
- [17] H. Takigawa, Y. Kitada, K. Shinagawa, R. Yuge, Y. Higashi, S. Tanaka, W. Yasui, K. Chayama, Multikinase inhibitor regorafenib inhibits the growth and metastasis of colon cancer with abundant stroma, *Canc. Sci.* 107 (2016) 601–608.
- [18] R. Yuge, Y. Kitada, H. Takigawa, T. Naito, N. Oue, W. Yasui, S. Tanaka, K. Chayama, Silencing of discoidin domain receptor-1 (DDR1) concurrently inhibits multiple steps of metastasis cascade in gastric cancer, *Transl Oncol* 11 (2018) 575–584.
- [19] T.F. Gajewski, The next hurdle in cancer immunotherapy: overcoming the non-T-cell-inflamed tumor microenvironment, *Semin. Oncol.* 42 (2015) 663–671.
- [20] P.S. Hegde, V. Karanikas, S. Evers, The where, the when, and the how of immune monitoring for cancer immunotherapies in the era of checkpoint inhibition, *Clin. Canc. Res.* 22 (2016) 1865–1874.
- [21] F. Pages, B. Mlecnik, F. Marliot, G. Bindea, F.S. Ou, C. Bifulco, A. Lugli, I. Zlobec, T. Rau, M.D. Berger, I.D. Nagtegaal, E. Vink-Börger, A. Hartmann, C. Geppert, J. Kolwelter, S. Merkel, R. Grützmann, M. Van den Eynde, A. Jouret-Mourin, A. Kartheuser, D. Léonard, C. Remue, J.Y. Wang, P. Bavi, M.H.A. Roehrl, P. S. Ohashi, L.T. Nguyen, S. Han, H.L. MacGregor, S. Hafezi-Bakhtiari, B.G. Wouters, G.V. Masucci, E.K. Andersson, E. Zavadova, M. Vocka, J. Spacek, L. Petruzella, B. Konopasek, P. Dunder, H. Skalova, K. Nemejcova, G. Botti, F. Tatangelo, P. Delrio, G. Ciliberto, M. Maio, L. Laghi, F. Grizzi, T. Fredriksen, B. Buttard, M. Angelova, A. Vasaturo, P. Maby, S.E. Church, H.K. Angell, L. Lafontaine, D. Bruni, C. El Sissy, N. Haicheur, A. Kirilovsky, A. Berger, C. Lagorce, J.P. Meyers, C. Paustian, Z. Feng, C. Ballesteros-Merino, J. Dijkstra, C. van de Water, S. van Lent-van Vliet, N. Knijn, A. Muşină, D. Scripcariu, B. Popivanova, M. Xu, T. Fujita, S. Hazama, N. Suzuki, H. Nagano, K. Okuno, T. Toriogo, N. Sato, T. Furuhashi, I. Takemasa, K. Itoh, P. S. Patel, H.H. Vora, B. Shah, J.B. Patel, K.N. Rajvik, S.J. Pandya, S.N. Shukla, Y. Wang, G. Zhang, Y. Kawakami, F.M. Marincola, P.A. Ascierto, D.J. Sargent, B. A. Fox, J. Galon, International validation of the consensus Immunoscore for the classification of colon cancer: a prognostic and accuracy study, *Lancet* 391 (2018) 2128–2139.
- [22] E. Lanitis, M. Irving, G. Coukos, Targeting the tumor vasculature to enhance T cell activity, *Curr. Opin. Immunol.* 33 (2015) 55–63.
- [23] L.Y. Tan, C. Martini, Z.G. Fridlender, C.S. Bonder, M.P. Brown, L.M. Ebert, Control of immune cell entry through the tumour vasculature: a missing link in optimising melanoma immunotherapy? *Clin Transl Immunol* 6 (2017) e134.
- [24] N. Nagarsheth, M.S. Wicha, W. Zou, Chemokines in the cancer microenvironment and their relevance in cancer immunotherapy, *Nat. Rev. Immunol.* 17 (2017) 559–572.
- [25] M. Camus, M. Tosolini, B. Mlecnik, F. Pages, A. Kirilovsky, A. Berger, A. Costes, G. Bindea, P. Charoentong, P. Bruneval, Z. Trajanoski, W.-H. Fridman, J. Galon, Coordination of intratumoral immune reaction and human colorectal cancer recurrence, *Canc. Res.* 69 (2009) 2685–2693.
- [26] H. Tang, Y. Wang, L.K. Chlewicki, Y. Zhang, J. Guo, W. Liang, J. Wang, X. Wang, Y.-X. Fu, Facilitating T cell infiltration in tumor microenvironment overcomes resistance to PD-L1 blockade, *Canc. Cell* 29 (2016) 285–296.
- [27] T. Sumida, Y. Kitada, K. Shinagawa, M. Tanaka, M. Kodama, M. Ohnishi, E. Ohara, S. Tanaka, W. Yasui, K. Chayama, Anti-stromal therapy with imatinib inhibits growth and metastasis of gastric carcinoma in an orthotopic nude mouse model, *Int. J. Canc.* 128 (2011) 2050–2062.
- [28] E. Vilar, S.B. Gruber, Microsatellite instability in colorectal cancer—the stable evidence, *Nat. Rev. Clin. Oncol.* 7 (2010) 153–162.
- [29] N.M. Lindor, L.J. Burgart, O. Leontovich, R.M. Goldberg, J.M. Cunningham, D. J. Sargent, C. Walsh-Vockley, G.M. Petersen, M.D. Walsh, B.A. Leggett, J.P. Young, M.A. Barker, J.R. Jass, J. Hopper, S. Gallinger, B. Bapat, M. Redston, S. N. Thibodeau, Immunohistochemistry versus microsatellite instability testing in phenotyping colorectal tumors, *J. Clin. Oncol.* 20 (2002) 1043–1048.
- [30] T.C. Smyrk, P. Watson, K. Kaul, H.T. Lynch, Tumor-infiltrating lymphocytes are a marker for microsatellite instability in colorectal carcinoma, *Cancer* 91 (2001) 2417–2422.
- [31] *Proc. Natl. Acad. Sci. U. S. A.* 102 (2005) 15545–15550.
- [32] P.C. Tumeh, C.L. Harview, J.H. Yearly, I.P. Shintaku, E.J.M. Taylor, L. Robert, B. Chmielowski, M. Spasic, G. Henry, V. Ciobanu, A.N. West, M. Carmona, C. Kivork, E. Seja, G. Cherry, A.J. Gutierrez, T.R. Grogan, C. Mateus, G. Tomasic, J. A. Glaspy, R.O. Emerson, H. Robins, R.H. Pierce, D.A. Elashoff, C. Robert, A. Ribas, PD-1 blockade induces responses by inhibiting adaptive immune resistance, *Nature* 515 (2014) 568–571.
- [33] S. Spranger, R. Bao, T.F. Gajewski, Melanoma-intrinsic beta-catenin signalling prevents anti-tumour immunity, *Nature* 523 (2015) 231–235.
- [34] T. Iwata-Kajihara, H. Sumimoto, N. Kawamura, R. Ueda, T. Takahashi, H. Mizuguchi, M. Miyagishi, K. Takeda, Y. Kawakami, Enhanced cancer immunotherapy using STAT3-depleted dendritic cells with high Th1-inducing ability and resistance to cancer cell-derived inhibitory factors, *J. Immunol.* 187 (2011) 27–36.
- [35] B. Mlecnik, G. Bindea, H.K. Angell, P. Maby, M. Angelova, D. Tougeron, S. E. Church, L. Lafontaine, M. Fischer, T. Fredriksen, M. Sasso, A.M. Bilocq, A. Kirilovsky, A.C. Obenauf, M. Hamieh, A. Berger, P. Bruneval, J.-J. Tuche, J.-C. Sabourin, F. Le Pessot, J. Mauillon, A. Rafii, P. Laurent-Puig, M.R. Speicher, Z. Trajanoski, P. Michel, R. Seseboue, T. Frebourg, F. Pages, V. Valge-Archer, J.-B. Latouche, J. Galon, Integrative analyses of colorectal cancer show immunoscore is a stronger predictor of patient survival than microsatellite instability, *Immunity* 44 (2016) 698–711.
- [36] D.S. Williams, M.J. Bird, R.N. Jorissen, Y.L. Yu, F. Walker, H.H. Zhang, E.C. Nice, BurgessAW, Nonsense mediated decay resistant mutations are a source of expressed mutant proteins in colon cancer cell lines with microsatellite instability, *PLoS One* 5 (2010), e16012.
- [37] D.T. Le, J.N. Uram, H. Wang, B. Bartlett, H. Kemberling, A. Eyring, N.S. Azad, D. Laheru, R.C. Donehower, T.S. Crocenzi, R.M. Goldberg, G.A. Fisher, J.J. Lee, T. F. Greten, M. Koshiji, S.P. Kang, R.A. Anders, J.R. Eshleman, B. Vogelstein, L. A. Diaz, Programmed death-1 blockade in mismatch repair deficient colorectal cancer, *J. Clin. Oncol.* 34 (15 suppl) (2016) 103.
- [38] J. Paulsson, T. Sjöblom, P. Mücke, F. Ponten, G. Landberg, C.-H. Heldin, J. Bergh, D. J. Brennan, K. Jirstrom, A. Östman, Prognostic significance of stromal platelet-derived growth factor beta-receptor expression in human breast cancer, *Am. J. Pathol.* 175 (2009) 334–341.
- [39] G. Lindmark, C. Sundberg, B. Glimelius, L. Pahlman, K. Rubin, B. Gerdin, Stromal expression of platelet-derived growth factor beta-receptor and platelet-derived growth factor B-chain in colorectal cancer, *Lab. Invest.* 69 (1993) 682–689.
- [40] H.N. Antoniades, T. Galanopoulos, J. Neville-Golden, C.J. O'Hara, Malignant epithelial cells in primary human lung carcinomas coexpress in vivo platelet-derived growth factor (PDGF) and PDGF receptor mRNAs and their protein products, *Proc. Natl. Acad. Sci. U.S.A.* 89 (1992) 3942–3946.
- [41] M. Onoyama, Y. Kitada, Y. Tanaka, R. Yuge, K. Shinagawa, S. Tanaka, W. Yasui, K. Chayama, Combining molecular targeted drugs to inhibit both cancer cells and activated stromal cells in gastric cancer, *Neoplasia* 15 (2013) 1391–1399.
- [42] K. Pietras, A. Östman, M. Sjöquist, E. Buchdunger, R.K. Reed, C.-H. Heldin, K. Rubin, Inhibition of platelet-derived growth factor receptors reduces interstitial hypertension and increases transcapillary transport in tumors, *Canc. Res.* 61 (2001) 2929–2934.
- [43] K. Pietras, Increasing tumor uptake of anticancer drugs with imatinib, *Semin. Oncol.* 31 (2004) 18–23.